Wireless Networks
https://doi.org/10.1007/s11276-018-01926-z

Minimum cost event driven WSN with spatial differentiated QoS requirements

Debanjan Sadhukhan[1] · **Seela Veerabhadreswara Rao**[1]

Abstract

In wireless sensor networks applications like rare-event detection, maximizing lifetime, minimizing end-to-end delay, and minimizing the network cost, are some of the most important quality of service requirements. In applications like disastrous or fire event detection, if an event is detected very close to the center facility, the event information should reach to the base-station much faster than an event detected far away. In this work, we are interested to find a minimum cost network for such applications. A stochastic approach is used to find the minimum cost network for given lifetime requirement and spatial differentiated delay constraints. We use Monte-Carlo simulations for validating our analysis. In order to show the effectiveness of our approach, we use network simulator-2 simulations.

Keywords Ad-hoc networks · Quality of service · Wireless sensor networks · NS2 simulation · Monte Carlo simulation

1 Introduction

In applications like tsunami detection, intrusion detection, forest-fire detection, and many more, sensors are deployed in hard-to-reach, remote areas to detect certain rare events. For such applications, most of the time the sensors remain idle until a critical event is detected. Once an event is detected, the event information is forwarded to the base-station within a strict or stringent delay. Hence, delay becomes a primary quality of service (QoS) requirement. Generally, the sensor nodes are equipped with unattended and limited battery power source. Hence, extending the lifetime (the time duration when the first node in the network depletes its energy completely), while satisfying end-to-end (e2e) delay[1] constraint, are essential QoS requirements in event-driven data-gathering. Energy consumption can be reduced using sleep/wake (s/w) scheduling strategies. In these strategies, the communication device is turned-off in an absence of critical events. In synchronous s/w scheduling, sensor nodes exchange synchronization messages and wake up synchronously to send or receive data-packets, whereas in asynchronous techniques, the sensor nodes wake up independently. Asynchronous techniques save more energy than synchronous techniques for rare event detection applications because of the additional energy needed for synchronization. Asynchronous techniques decrease energy consumption at the cost of increasing e2e delay. This is because the sender waits until its forwarding node wakes up [10]. In asynchronous s/w scheduling, if wake-up rate increases energy consumption increases and lifetime decreases, but the e2e delay decreases, and vice-versa. The clock-skew, the queuing-delay, and the wake-up rate may affect the e2e delay, but the most dominating factor is the wake-up rate. In order to minimize the delay incurred in asynchronous strategies, anycasting based packet forwarding techniques are

✉ Debanjan Sadhukhan
debanjan.sadhukhan1987@gmail.com

1 Computer Science and Engineering, Indian Institute of Technology Guwahati, Guwahati 781039, India

[1] The e2e delay of a node is defined as the average time a packet takes from the node to reach the base-station. Moreover, the e2e delay of the network is defined as the maximum e2e delay encountered by any node in the network.

Published online: 24 January 2019

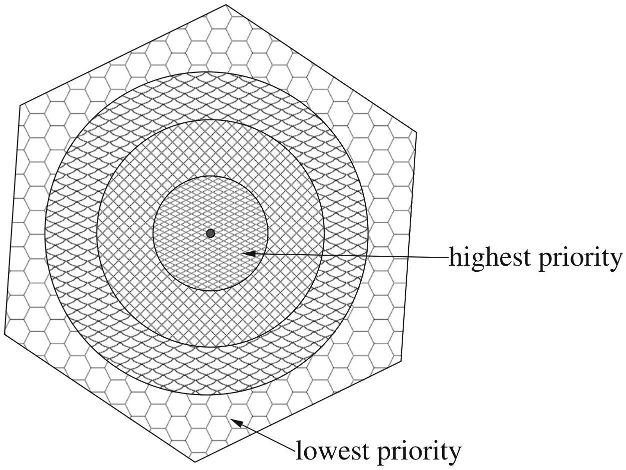

Fig. 1 Different priority areas

proposed in the literature. In anycasting based packet forwarding schemes, a sensor node considers a set of candidate nodes as forwarding nodes and at any time it forwards the data-packet to the first node wakes-up within this candidate set. Anycasting strategy reduces the expected waiting time compared to the strategy with a single forwarding node in conventional approaches.

In applications like disastrous of fire event detection, if an event is detected very close to the central facility then the event information needs to reach to the base-station very faster than an event detected far away. In other words, there can be a large variation in QoS requirements for different areas within the FoI. High priority areas are associated with stringent QoS requirements, whereas low priority areas are with relaxed QoS requirements. Assume the base-station along with the central facility is located in the middle of a convex-shaped FoI (refer Fig. 1). The area around the central facility is divided into circular rings with exponential e2e delay constraints like 1 ms, 10 ms, 100 ms, 1000 ms, 10,000 ms, etc. If an event is detected in an area with darker shade, the event information must reach to the base-station much faster than an event is detected in areas with lighter shades.

Designing a minimum cost network for such an application, while satisfying the delay constraints for each area and the lifetime requirement of the overall network, is an interesting problem. Hence, in this work we are interested in the problem: *finding a minimum cost WSN*[2] *for given spatial differentiated e2e delay constraints and lifetime requirement in a convex-shaped FoI.*

In the next section, we review the significant contributions that are proposed in the literature. In Sect. 3, we are interested to find a minimum cost network that satisfies both the spatial differentiated delay constraints and lifetime requirements. We use Monte Carlo simulation to validate our expected analysis. In the fourth section we analyze the effectiveness of our strategy using the NS2 simulation. The last section draws the conclusion of the paper.

2 Related work

This section gives a brief survey for various methods that addressed the problem of finding CSD and efficient event-driven data-gathering protocols designed for WSN.

The problem of finding CSD to satisfy given coverage requirement is well addressed in the literature [3, 6]. In [24], the authors estimated CSD for intrusion detection in the border patrol system. However, minimizing cost and delay is not addressed in this work. In [27], the authors further enhanced the coverage quality and detection accuracy by adding more nodes for such a system. Especially, the number of redundant nodes are calculated to satisfy the quality of coverage. A maritime border surveillance system was proposed in [18]. In this work, intrusion is detected by differentiating ocean waves and ship generated waves. For small vessel or ships, high density nodes are required to distinguish between ship waves and ocean waves, and hence this strategy is not cost effective. Recently, in [8] the authors proposed a method to calculate sensor density to achieve the desired level of coverage for intrusion detection in boarder monitoring systems. Their method also maintains good connectivity across the network. The authors also extended their approach to provide a novel cross layer routing protocol, while maintaining communication need and link reliability. In [20], the authors derived an upper bound on the lifetime for given density and degree of coverage.

A survey of various energy-efficient routing protocols is given in [26]. Clustering based approaches are proposed in [7, 23] where the sensor nodes aggregate data before forwarding to save energy. In order to minimize energy consumption further, duty-cycling (or s/w scheduling) is adopted in the literature. This approach reduces idle-listening where the sensor nodes keep the transceiver on even when no packets are expected to receive/send. A comparative study for different routing techniques with duty-cycling is given in [1]. These techniques can be categorized as synchronous or asynchronous. In order to save energy, in synchronous s/w scheduling each sender and receiver pair wakes up at the same time to exchange the data packets [11, 31]. These type of scheduling techniques require time-synchronization which increases energy consumption. Quorum based routing protocols are also proposed to minimize overall energy consumption [4, 5, 9, 15, 17, 25].

[2] In this paper we assume that solving the problem of minimum cost network is as same as finding the critical sensor density because the number of nodes is directly proportional to the overall deplyment cost of the network.

In asynchronous sleep/wake scheduling techniques, a sensor node wakes up independently. In rare-event detection applications, asynchronous techniques are applied because of overhead involved in synchronous techniques. In rare event detection, anycasting forwarding with asynchronous s/w scheduling is considered to be one of the best methods for minimizing the delay and maximizing the lifetime [16, 19, 21, 22].

The overall e2e delay of the forwarding set may increase if the recently added nodes have higher expected e2e delay. Based on this observation, an anycasting based forwarding scheme is proposed by Kim et al. where the neighboring nodes that can collectively minimize expected e2e delay are only added to the forwarding set [12]. When an event is detected, a longer route may be followed by the packet as because the forwarding node with shorter route is asleep. In order to mitigate this issue, a delay optimal anycasting scheme is developed by the same author in [13] where sensor nodes instead of forwarding the packet immediately, wait for some time and then opportunistically forwarded only when the expected delay is more than waiting.

Motivation and Contribution The problem of finding CSD is well addressed in the literature in the context of satisfying coverage and connectivity requirements [3, 6, 14, 28–30]. The method described in [20] derived an upper bound for lifetime of the WSN, but the problem of finding CSD is not addressed for given spatial differentiated delay constraints and lifetime requirement. The anycasting forwarding techniques [2, 12, 13, 16, 21, 22] discussed in the literature are not applicable to find the CSD for given spatial differentiated delay constraints and lifetime requirement.

In this paper, we are interested to find a minimum cost network that satisfies the spatial differentiated delay constraints of each area and the lifetime requirement of the overall network. In order to find the minimum cost network, the critical sensor density for each area is estimated. The major contributions for our work are as follows:

- We use stochastic approaches to estimate the expected e2e delay of a random node, for a given density, placed in an arbitrary distance from the base-station. We use the numerical iteration technique to estimate the expected e2e delay of the FoI by gradually increasing the distance of the random node from the base-station. We use this information to find the CSD required to satisfy the the lifetime requirement and the spatially differentiated delay constraints.
- We validate our analysis using Monte-Carlo simulation and show that the simulation results are close to our numerical estimation for various scenarios.
- The effectiveness of our approach is shown by giving a theoretical analysis. We also show the effectiveness using NS2 simulation in minimizing network cost and satisfying given constraints, for various cases.

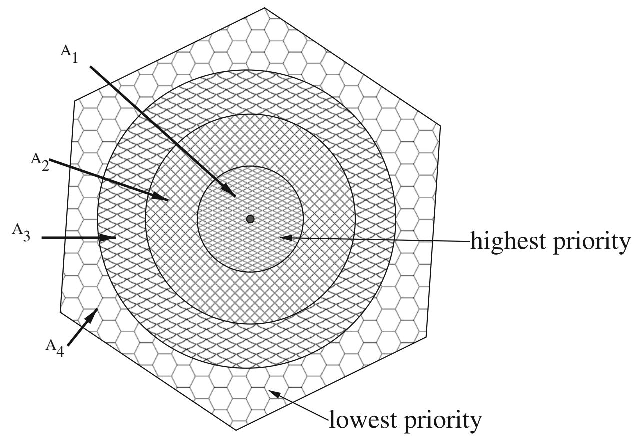

Fig. 2 Sensors are deployed at a rate λ_i uniform randomly in A_i, $1 \leq i \leq n$, where $n = 4$. This example also shows A_1 is the closest area to the base-station, A_2 is closer than A_3, A_3 is closer than A_4. If $i < j$, then A_i is closer to the base-station than A_j

3 Minimum cost network for spatial differentiated QoS

Assume the FoI, A, is partitioned into different areas A_i such that each A_i is associated with delay constraint D_i and lifetime constraint L_c (refer Fig. 2). Moreover, the area of each A_i is denoted as $||A_i||$ such that $||A|| = \sum_{i=1}^{n} ||A_i||$, where n denotes the number of partitioned areas. Sensor nodes are deployed uniform randomly[3] in A_i with density λ_i. If c denotes the cost of each sensor, then the overall cost of deployment is $\sum_{i=1}^{n} ||A_i|| \times \lambda_i \times c$. Hence, our objective of this work is to estimate critical sensor densities, λ_i, for each A_i, that minimizes overall deployment cost.

Assume sensor nodes wake-up periodically at a rate w. In other words, sensor nodes monitor the medium at an interval of $\frac{1}{w}$ to check if any neighboring node is trying to transmit any critical information. If a sensor node detects a critical information (like fire or tsunami), it waits until any eligible forwarding node wakes up. Assuming E denotes the sum of energy required for the state transition from sleep to wake-up and energy required during wake-up, average lifetime can be denoted as $L_f = \frac{Q}{w \times E}$, where Q denotes the initial energy available in sensor nodes. Hence, for a given lifetime requirement L_c, we can estimate average wake-up rate as $w = \frac{Q}{L_c \times w}$.

[3] This kind of deployment can be justified when the sensor nodes are air-dropped from a plane in a hostile environment.

A stochastic approach is used in this work to find the minimum cost network for given delay constraints and lifetime requirement. We first estimate the expected e2e delay for a random density, and use this information to estimate the CSD λ_i , for each $i \in n$, that minimizes overall cost (refer Fig. 2). We estimate the CSD of each area in increasing order of distance $(A_1, A_2, \ldots, A_n)$ in our strategy, to estimate the overall minimum cost network of the FoI.

If density increases, expected e2e delay decreases and vice versa. Moreover, if density increases the overall cost of the network increases as well. Hence, in this work our objective is to estimate the CSD that satisfies the delay constraint. In order to find the relation between sensor density and expected e2e delay, we derive expressions involve sensor density and e2e delay in Sect. 3.1. Sect. 3.1 discusses details about estimating e2e delay for a sensor density λ. We use these expressions to estimate a minimum cost network. Section 3.3 discusses details about estimating minimum cost network. When the CSD for each area A_i is estimated, sensor nodes can be deployed over the respective area using estimated density $\lambda_i, 1 \le i \le n$, to satisfy the delay constraints and lifetime requirement.

3.1 Expected e2e delay

Expected e2e delay of the network is the maximum of the expected e2e delay encountered by any node present in the network, which is the farthest node. We first assume that the FoI is circular and then find the expected e2e delay for a node located at the perimeter. We extend this strategy for a convex-shaped FoI.

Note that the expected e2e delay for a random node, say i, depends on the expected e2e delay of the neighboring nodes of i. In other words, the e2e delay depends on the neighboring node which forwards the packet to the base-station. If the e2e delay of the neighbors of i is high then the e2e delay of node i is also high. To estimate the expected e2e delay of the node i located at the perimeter, we estimate the expected e2e delay for the nodes located closer from the base-station. In other words, first we estimate the expected e2e delay for a randomly chosen node and then slowly increase the distance of this node from the base-station. For estimating the expected e2e delay for a random located in the perimeter, we increase the distance till we reach at the perimeter (refer Fig. 3).

3.1.1 Expected e2e delay for a random node *i*

Assume sensor nodes are deployed uniform randomly. $A(i, C)$ denotes the (circular) region with radius C such that the circle is centered at the node i so that the sensor node i can directly communicate to any node located within the

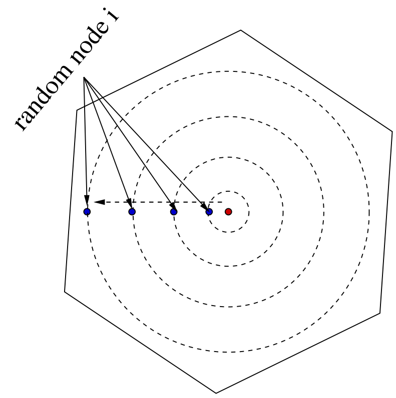

Fig. 3 We increase the distance of a random node, say i, gradually from the base-station to estimate the expected e2e delay

region $A(i, C)$.[4] Consider a random node i, before transmitting the data packet, the node i transmits a beacon signal which is of duration t_B, then an ID signal which is of duration t_C, and then the node listens for any acknowledgment and waits for the duration of t_A (refer Fig. 4). A node sends acknowledgement if it hears the beacon and belongs to the forwarding set of i, F_i. Let w be the asynchronous periodic wake-up rate. If $F_i = \{i_1, i_2, \ldots, i_k\}$, such that k denotes the number of nodes present in the forwarding set, then the probability of a node in F_i wakes up at hth beacon is $p_w = \frac{t_I}{1/w}$, if $h < \frac{1/w}{t_I}$, else 1, where $t_I = t_A + t_B + t_C$ denotes the beacon interval.

Let W denotes the event that the corresponding forwarding nodes in the forwarding set wake up in their respective beacons. Consider an example $W = \{1, 4, 5, \ldots, 10\}$ that denotes node 1 wakes up at the 1st beacon, node 2 wakes up at the 4th beacon, node 3 at 5th beacon and so on. $P(W) = (p_w)^k$ denotes the probability for the event W, where k is the cardinality of F_i. Let X denotes an event where no nodes wakes up for first $h-1$ beacon signals and j number of nodes actually wake up at hth beacon signal, and the rest of $k-j$ number of nodes can wake up in the last $h_{max} - h$ beacon signals. Moreover, $h_{max} = \frac{1/w}{t_I}$ be the total number of possible beacons. $P(X)$, the probability for the event X, is denoted by

$$P(X) = {}^k C_j (h_{max} - h)^{k-j} (p_w)^k, \tag{1}$$

since ${}^k C_j$ number of possible sets where different nodes wake up in hth beacon and rest, $k-j$, nodes can wake up for $(h_{max} - h)$ beacons in $(h_{max} - h)^{k-j}$ different ways.

Note that, a packet is forwarded after h beacons only when at least a single node wakes up in hth beacon provided no node can wake up during $(h-1)$ beacons and all

[4] Note that, a sensor node may not directly communicate to base-station, but multi-hop communication can be used to send the data-packet to he base-station.

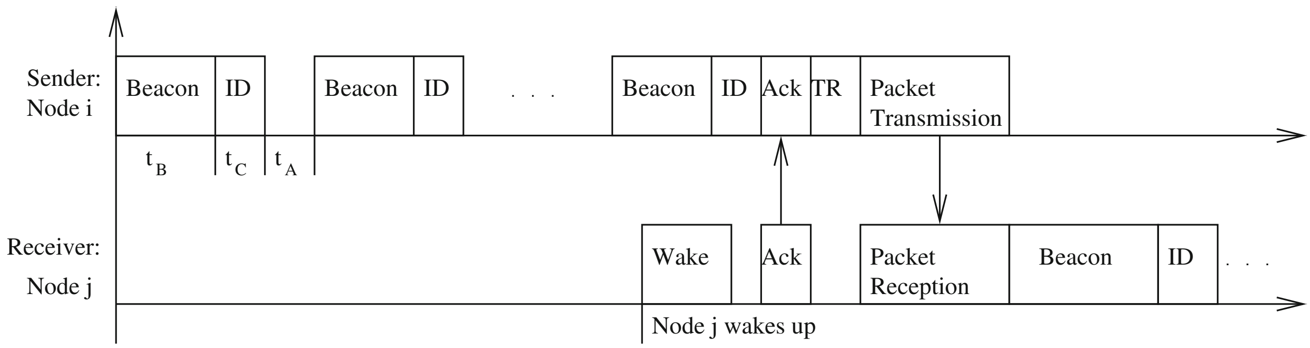

Fig. 4 Packet forwarding protocol

remaining nodes can wake-up in the remaining $(h_{max} - h)$. Let W_h denotes the event for no node actually wake up in $(h-1)$ beacon signals, at-least a single node wakes up at the hth signal, and rest of the nodes can wake up in the last $(h_{max} - h)$ beacons, such that the packet is actually forwarded at hth beacon signal. Hence, the corresponding probability, $P(W_h)$, that the packet is forwarded to atleast one forwarding node at hth beacon signal, is given by,

$$P(W_h) = \sum_{j=1}^{k} {}^{k}C_j (h_{max} - h)^{k-j} (p_w)^k, \tag{2}$$

since there are a total of k nodes present within the forwarding set. Hence, we can find the expected one hop delay as

$$d_{k,w} = \sum_{h=1}^{\left\lfloor \frac{1/w}{t_I} \right\rfloor} P(W_h) * h + t_D, \tag{3}$$

where the transmission delay is denoted by t_D. Consider a node i. Note that, the expected e2e delay is nothing but the sum of the expected e2e delay of the nodes that are present in the forwarding set F_i and the (expected) one hop delay of node i. Note that $\frac{1}{k}$ is nothing but the probability for a packet which is forwarded to any node j present within F_i where k denotes the cardinality of F_i. Hence, the following lemma continues.

Lemma 1 *Let* $\{i_1, i_2, \ldots, i_k\}$ *denotes the forwarding set for the node i. If the expected e2e delay for the node* $i_j \in F_i$ *is denoted by* $D_{i_j,k,w}$ *for* $1 \le j \le k$, *the expected e2e delay for node i is* $D_{i,k,w} = d_{k,w} + \sum_{j=1}^{k} \frac{1}{k} * D_{i_j,k,w}$, *such that* $d_{k,w} = \sum_{h=1}^{\left\lfloor \frac{1/w}{t_I} \right\rfloor} P(W_{h,k}) * h + t_D$.

Using Lemma 1, expected e2e delay for the node i can be estimated. Assuming the expected e2e delay for the nodes present in the forwarding set, F_i, is known, we can estimate e2e delay for the randomly chosen node i using Lemma 1. In the next subsection we use this information and estimate the e2e delay of a circular-shaped FoI.

3.1.2 Expected e2e delay for a FoI

In Sect. 3.1.1, we estimated expected e2e delay for a random node i. In this sub-section, we find the expected e2e delay for a circular shaped FoI by increasing the distance for a random node i.

As because the base-station remains always awake, any node which can directly communicate to the base-station has e2e delay as the same as the transmission delay t_D.[5] This direct communication region is denoted by the circle C_D. This is because, we assume the communication device of the base-station is always switched on. Now we use this information to find the e2e delay for a random node $i \notin C_D$.

Assume, the FoI is divided in rings of concentric circles. We first find the e2e delay for a random node in each of the circular rings and then use it to estimate the expected e2e delay of the farthest ring. We use the e2e delay for the nodes within C_D to find the expected e2e delay of a random node that belongs to the first ring. Consider b_p denotes the location where the base-station is placed. Expected e2e delay of a random node i that belongs to the circular annulus (CA), $CA(b_p, C, C + \delta_1)$, is estimated such that the neighbors of node i is in C_D. The CA, $CA(b_p, R_i, R_j)$, is an area which is defined as the difference between the boundaries of the circles centered at b_p with radii R_i and R_j. To estimate the expected e2e delay for a node i, the notion of effective forwarding region of communication (EFC) is introduced.

$$\begin{aligned} CI(dis_i, \delta) = {} & 2\cos^{-1}\left(\frac{\delta^2 - c^2 - 2dis_i\delta}{2dis_i C}\right) C^2 - \frac{\delta^2 - c^2 - 2dis_i\delta}{2dis_i} \\ & \times \sqrt{C^2 - \left(\frac{\delta^2 - c^2 - 2dis_i\delta}{2dis_i}\right)^2} + 2\cos^{-1}\left(\frac{dis_i - \frac{\delta^2 - c^2 - 2dis_i\delta}{2dis_i}}{dis_i - \delta}\right) C^2 \\ & - \left(dis_i - \frac{\delta^2 - c^2 - 2dis_i\delta}{2dis_i}\right) \times \sqrt{C^2 - \left(\frac{\delta^2 - c^2 - 2dis_i\delta}{2dis_i}\right)^2} \end{aligned} \tag{4}$$

[5] Note that, t_D denotes the average transmission delay without accounting the randomness involved in wireless channel.

Fig. 5 E2e delay in a circular-shaped FoI

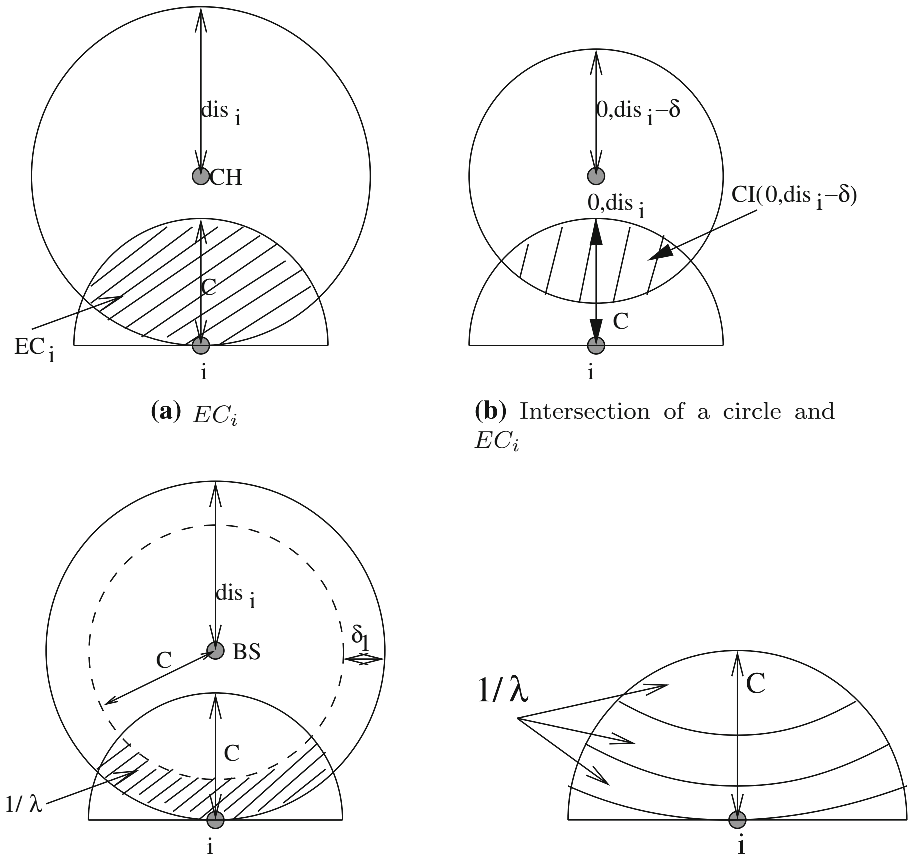

(a) EC_i

(b) Intersection of a circle and EC_i

(c) One node is expected in the shaded region

(d) EC_i is divided into equal area sectoral annuli.

Consider a node i which is placed at a location distance dis_i from the base station. The intersection of the communication region of node i and the open circular area of radius dis_i that is centered at the base-station can be denoted as EFC and is denoted by EC_i (refer Fig. 5a). Note that the neighbors belong to EC_i are only eligible to forward a data-packet to the base-station as these nodes are located closer to the base-station. Following lemma quantifies the area of EC_i.

Lemma 2 *Consider a node i with a communication range C and placed at a distance of dis_i, such that $dis_i > C$, from base-station. The area for the EFC, EC_i, is* $||EC_i|| = 2\cos^{-1}\left(\frac{C}{2dis_i}\right)C^2 + 2\cos^{-1}\left(1 - \frac{C^2}{2dis_i^{\,2}}\right)dis_i^{\,2} - dis_i \sqrt{C^2 - \left(\frac{C^2}{2dis_i}\right)^2}$.

The above lemma can be proved by using simple geometry. To estimate the expected e2e delay the area formed by the intersection of the EFC and the circle centered at the base-station is estimated. We estimate the intersection of the EC_i and a circle that is centered at the base-station for node i as follows.

Lemma 3 *Assume a node i, with communication range C, is placed dis_i distance from the base station. The intersection of the EFC, EC_i, and a circle which is centered at the base-station (b_p) such that the circle has radius $R_j = dis_i - \delta, 0 < \delta \leq C$, $CI(dis_i, \delta)$, is given by Eq. 4 (see Fig. 5b).*

Now we are ready to find the expected e2e delay of the closest CA. Later we extend this strategy to find the expected e2e delay of the farther CA. Consider a random node i which is located inside the CA, $CA(b_p, C, C + \delta_1)$, so that EC_i contains the neighbors that can communicate with base-station directly. Assume the maximum width of such a circular annulus $CA(b_p, C, C + \delta_1)$ is given by δ_1. Consider the shaded area in Fig 5(c) where it is expected that only one node is located that is nothing but the node i. Then, in Fig 5(c) the area expected within the shaded region can be given by $\frac{1}{\lambda}$, where node density is denoted by λ. We use the following equation to find the expected maximum value of δ_1.

$$EC_i - CI(dis_i, \delta_1) = \frac{1}{\lambda}. \tag{5}$$

Equation 5 is a single variable equation, hence we can assume it is solved in constant time. In order to estimate the expected e2e delay for a node that belongs to the CA $CA(b_p, C, C+\delta_1)$, we use the lemma as follows.

Lemma 4 *Consider a node i that lies inside the CA $CA(b_p, C, C+\delta_1)$. Assume that the EFC, EC_i, only contains the neighbors which are within the direct communication circle, C_D. The expected e2e delay for a node i can be given by $D_{i,k,w} = \sum_{h=1}^{\left\lfloor \frac{1/w}{t_l} \right\rfloor} p_{h,k,w} * h + t_D$, where λ is the node density and $k = EC_i * \lambda - 1$.*

Proof Note that the neighboring nodes within the set of forwarding node i, F_i, are expected to lie within the area of $||EC_i|| * \lambda - 1$ (refer Fig 5c). Since these nodes can communicate to the base-station directly, the expected e2e delay of these nodes is t_D. To minimize the overall e2e delay for node i, all neighbors within EC_i are included inside F_i. Hence, the expected e2e delay of node i can be given by $D_{i,k,w} = \sum_{h=1}^{\left\lfloor \frac{1/w}{t_l} \right\rfloor} p_{h,k,w} * h + t_D$, where $k = ||EC_i|| * \lambda - 1$. □

To estimate the expected e2e delay for the FoI, we raise the distance of the node i from the base-station by γ gradually and estimate the exp e2e delay. The expected e2e delay of the nodes in $C + \delta_1 + (m-1)\gamma$ is used to estimate the expected e2e delay of the node i at a distance $C + \delta_1 + m\gamma$. To estimate the e2e delay for node i, we partition EC_i of node i in a set of sectoral annuli so that each sectoral annulus (SA) contains only one node (refer Fig. 5d), such that $1 \le j \le k$, and $k = ||EC_i|| * \lambda - 1$. Consider a node i. The jth SA, $SA_{i,j}(\beta_{i_{j1}}, \beta_{i_{j2}})$, of the node i can be defined as the intersection of the two concentric circles, centered at b_p that have radii $\beta_{i_{j1}}$ and $\beta_{i_{j2}}$ respectively, such that $\beta_{i_{j1}} > \beta_{i_{j2}}$. Assume the nearest SA from the base-station is i_1. Moreover, $\beta_{i_{11}}$ is same as $dis_i - C$. Hence, the following equation can be solved to estimate $\beta_{i_{12}}$.

$$CI(dis_i, \beta_{i_{12}} - (dis_i - C)) = \frac{1}{\lambda}. \tag{6}$$

Moreover, $\beta_{i_{21}} = \beta_{i_{12}}$ and $\beta_{i_{j1}} = \beta_{i_{(j-1)}2}$, for $2 \le j \le k$. $\beta_{i_{j2}}$, for any i_j, can be calculated as

$$CI(dis_i, \beta_{i_{j2}} - \beta_{i_{j1}}) = \frac{1}{\lambda}, \tag{7}$$

where $1 \le j \le k$. Assuming the Eqs. 6 and 7 is solvable in constant time because of the fact that these equations are single variable. In order to find the e2e delay for a randomly chosen node i, we use the estimation of the expected e2e delay for a random node that is belonged to jth SA.

Assume a random SA, $SA_{i,j}(\beta_{i_{j1}}, \beta_{i_{j2}})$. Also assume that m_{i_1} is the largest integer so that $C + \delta_1 + m_{i_1}\gamma \le \beta_{i_{j1}}$. We also assume that m_{i_2} be the smallest integer such that $C + \delta_1 + m_{i_2}\gamma \ge \beta_{i_{j2}}$. To estimate the e2e delay for a randomly chosen node in $SA_{i,j}(\beta_{i_{j1}}, \beta_{i_{j2}})$, the estimated expected e2e delay of the nodes at the distances $C + \delta_1 + (m_{i_1}+1)\gamma, C + \delta_1 + (m_{i_1}+2)\gamma, \ldots, C + \delta_1 + m_{i_2}\gamma$ is used. Note that the node can present in any one of the areas generated by the intersection between the ring that is formed by the CA, $CA(b_p, C + \delta_1 + t\gamma, C + \delta_1 + (t+1)\gamma)$, and $SA_{i,j}(\beta_{i_{j1}}, \beta_{i_{j2}})$, where $m_{i_1} \le t \le (m_{i_2} - 1)$. The expected e2e delay for a randomly chosen node within $SA_{i,j}(\beta_{i_{j1}}, \beta_{i_{j2}})$ depends on the area generated by the intersection between the ring generated by the corresponding circular annuli and $SA_{i,j}(\beta_{i_{j1}}, \beta_{i_{j2}})$.

$$\begin{aligned} &||SA_{i,j}(C + \delta_1 + t\gamma, C + \delta_1 + (t+1)\gamma)|| \\ &= CI(dis_i, dis_i - (C + \delta_1 + t\gamma)) \\ &\quad - \sum_{s=1}^{t-1} \left\|SA_{i,j}(C + \delta_1 + s\gamma, C + \delta_1 + (s+1)\gamma)\right\| - \frac{1}{\lambda}(k-j). \end{aligned} \tag{8}$$

Note that, $CI(dis_i, dis_i - (C + \delta_1 + (m_{i_1}+1)\gamma)) - \frac{1}{\lambda}(k - j)$ is the area induced that is by $SA_{i,j}(C + \delta_1 + m_{i_1}\gamma, C + \delta_1 + (m_{i_1}+1)\gamma)$. The Eq. 8 denotes the area which is induced by $SA_{i,j}(C + \delta_1 + t\gamma, C + \delta_1 + (t+1)\gamma)$ for $m_{i_1} < t \le (m_{i_2} - 1)$. Also note that $||SA_{i,j}(C + \delta_1 + t\gamma, C + \delta_1 + (t+1)\gamma)||\lambda$ denotes the probability of node i_j belongs within $SA_{i,j}(C + \delta_1 + t\gamma, C + \delta_1 + (t+1)\gamma)$. Assume the minimum expected e2e delay for a randomly chosen node in $SA_{i,j}(C + \delta_1 + t\gamma, C + \delta_1 + (t+1)\gamma)$ is denoted by $D_{i_j,t\gamma}$. An upper bound for the expected e2e delay for the node i_j, D_{i_j}, can be given by $\sum_{t=m_{i_1}}^{(m_{i_2}-1)} ||SA_{i,j}(C + \delta_1 + t\gamma, C + \delta_1 + (t+1)\gamma)||\lambda D_{i_j,t\gamma}$.

To estimate the expected e2e delay of a random node i which is placed at a distance $dis_i = C + \delta_1 + m\gamma$, the expected e2e delay D_{i_j} for the random nodes belong to i_jth SA, for all j, are used. Assume a randomly selected node i located $dis_i = C + \delta_1 + m\gamma$ distant from the base-station. To find the expected e2e delay, the EC_i is divided into $EC_i * \lambda - 1$ SA such that it is expected every SA contains only one node. The expected e2e delay, of a node that belongs to the CA i_j, for $1 \le j \le (EC_i * \lambda - 1)$, can be estimated from the e2e delays of the nodes that are located at $C + \delta_1 + \gamma, C + \delta_1 + 2\gamma, \ldots, C + \delta_1 + (m-1)\gamma$ distant and is denoted by D_{i_j}. In order to minimize the overall e2e delay, we linearly search the nodes that belongs to every SA, while giving more priority for the nodes that are more closer with respect to the base-station, is used to find effectively k' which denotes the required forwarding set of nodes [12]. Hence, we can upper-bound the e2e delay for the node i as $D_{i,k',w} = d_{k',w} + \sum_{j=1}^{k'} \frac{1}{k'} * D_{i_j}$, where $d_{k',w} = \sum_{h=1}^{\left\lfloor \frac{1/w}{t_I} \right\rfloor} P(W_{h,k'}) * h + t_D$. Hence, we can write the following theorem.

$$
\begin{aligned}
||ECR_i^{q_0\,q_1\,q_2\,q_3\,q_4}|| = {} & 2\cos^{-1}\left(1 - \frac{C^2}{2{dis_i}^2}\right){dis_i}^2 \\
& - dis_i\sqrt{C^2 - \left(\frac{C^2}{2dis_i}\right)^2} + \left(cos^{-1}\left(\frac{y_3}{C}\right) + cos^{-1}\left(\frac{C}{2dis_i}\right)\right)C^2 \\
& + \triangle(q_3, q_4, q_0) + \left(\cos^{-1}\frac{dis_i - y_4}{dis_i}\right){dis_i}^2 \\
& - \left(\frac{1}{2}x_4 dis_i\right).
\end{aligned} \tag{9}
$$

Theorem 1 *Consider, i_j denotes a node within the CA $SA_{i,j}(\beta_{i_{j1}}, \beta_{i_{j2}})$ for node i so that i is located at a distance of $dis_i = C + \delta_1 + m\gamma$ from the base station. Let the estimated expected e2e delay of node i_j is denoted by D_{i_j}, for all $1 \leq j \leq (EC_i * \lambda - 1)$. If the forwarding set contains k' nodes, then we can upper-bound the minimum expected e2e delay for node i as $D_{i,k',w} = d_{k',w} + \sum_{j=1}^{k'} \frac{1}{k'} * D_{i_j}$, where $d_{k',w} = \sum_{h=1}^{\left\lfloor \frac{1/w}{t_I} \right\rfloor} P(W_{h,k'}) * h + t_D$.*

Now we are ready to estimate the e2e delay for a circular-FoI. We gradually increase distance of a randomly selected node i, in γ steps, such that $dis_i > \delta_1$, and the maximum e2e delay in a circular-FoI is estimated. We continue this process till the furthest point is reached which is nothing but the radius of the FoI. We showed the overall procedure in Algorithm 1.

3.1.3 Estimation of expected e2e delay of a convex-FoI

Consider a FoI which is convex-shaped and is denoted by $A = \langle p_1, p_2, p_3, p_4, p_5 \rangle$, as shown in Fig. 6(a), such that the base-station is located at b_p. Let r_A be the radius of the largest inscribed circle C_{b_p} inside A. The maximum expected e2e delay of C_{b_p} can be found using Algorithm 1. The steps for calculating the expected e2e delay of a node $i \in A - C_{b_p}$ is similar to Sect. 3.1.2 except the boundary of the FoI intersects EC_i and $CI(dis_i, \delta)$. In this subsection we show how EC_i and $CI(dis_i, \delta)$ can be estimated for a node $i \in A - C_{b_p}$.

The new EFC of the node i is the intersection of EC_i and A. There are three cases depending on the number of edges of the convex polygon A intersecting EC_i (refer Fig. 6a).

Case 1: If no edge is intersecting, then the new EFC is same as EC_i.

Case 2: If the new EFC is cut by only one edge of A as shown in Fig. 6(b), then it is estimated using the following method. Assume $\overline{a\,b}$ and $\widehat{a\,b\,c}$ respectively denotes the line segment that joins the points a and b, and the arc joining points a, b and c in counter clock-wise direction. Hence, the line segment $\overline{p_1\,p_2}$ cuts EC_i at q_3 and q_4. Let (x_i, y_i) be the co-ordinates of q_i. The new EFC, $ECR_i^{q_0\,q_1\,q_2\,q_3\,q_4}$, is enclosed between the line segment $\overline{q_3\,q_4}$, arc $q_4\widehat{q_0}q_1$, and arc $q_1\widehat{q_2}q_3$. Hence, the area $||ECR_i^{q_0\,q_1\,q_2\,q_3\,q_4}||$ can be found using Equation 9, which can be verified by simple geometry.

Case 3: If EC_i is cut by two line segments of different sides of FoI as shown in Fig. 6(c), then the EFC is enclosed between the line segment $\overline{q_4\,q_5}$, arc $q_5\widehat{q_0}q_1$, line segment

---

Algorithm 1: Estimates maximum e2e delay of a circular shaped FoI with radius r

---

Output: D_r: Maximum e2e delay in the FoI with radius r

Estimate t_D, δ_1 using Lemma 4

Set $m = 1$ and the distance of node i from base-station $dis_i = \delta_1$

do

  Set $dis_i = m\gamma + \delta_1$

  Find the required number of nodes (k') that minimizes e2e delay in EC_i using linear search

  Estimate expected e2e delay $D_{i,k',w}$ using Theorem 1

  $m++$

while $dis_i \leq r$

$D_{i,k',w} = D_r$

Fig. 6 EC_i is intersected by FoI

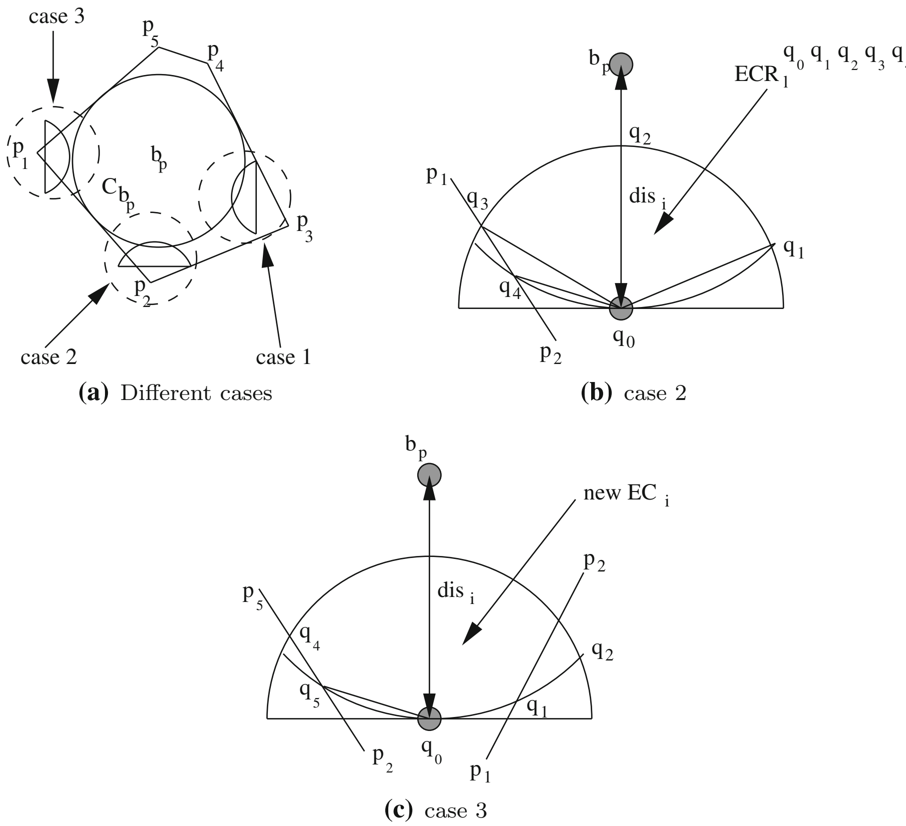

(a) Different cases

(b) case 2

(c) case 3

$\overline{q_1 q_2}$, and arc $q_2 \widehat{q_3} q_4$, which can also be found using the similar method.

Now we estimate the area of intersection of a circle centered at the base-station and the EFC of a random node. In a similar way, there are three possible cases depending on the number of edges of the polygon A intersecting $CI(dis_i, \delta)$ (see Fig. 7a).

Case 1: When $CI(dis_i, \delta)$ is not intersected by an edge of A, then it is same as $CI(dis_i, \delta)$.

Case 2: If $CI(dis_i, \delta)$ is intersected by one edge (refer Fig. 7b), then the area is enclosed between the line segment $\overline{q_4 q_5}$, arc $q_5 \widehat{q_1} q_2$, and arc $q_2 \widehat{q_3} q_4$. Using simple geometry this area can be calculated.

Case 3: Similarly, if $CI(dis_i, \delta)$ is cut by two line segments of two different sides of FoI (see Fig. 7c), then the intersected area is bounded by the line segment $\overline{q_5 q_6}$, arc $q_6 \widehat{q_1} q_2$, line segment $\overline{q_2 q_3}$, and arc $q_3 \widehat{q_4} q_5$ (Fig. 8).

Now we can find the e2e delay for a random node $i \in A - C_{b_p}$. Depending on the position of node i, expected e2e delay changes within the same CA, because the EFC and the e2e delay of the next-hop nodes change within the same CA. As mentioned earlier, the FoI is divided into several circular annuli in the steps of γ. Moreover, we further divide each CA into several parts, in the steps of δ, as shown in Fig. 9.

To estimate the e2e delay for a node within each SA, we divide each SA into several small parts of size δ as shown in Fig. 9. Assuming the expected e2e delay D_{δ_l}, of the node within the sub part δ_l of size $||\delta_l||$, within the jth SA of size $||SA_{i,j}||$ is known, one can find the expected e2e delay, $D_{i,j}$, of a random node within jth SA, using the following equation.

$$D_{i,j} = \sum_{\forall l} \frac{||\delta_l||}{||SA_{i,j}||} \times D_{\delta_l}. \tag{10}$$

The overall procedure is depicted in Algorithm 2.

Algorithm 2: Estimates maximum e2e delay of a convex-shaped FoI

```
Using Algorithm 1 estimate e2e delay of C_{b_p}
Set m = 1, p = 1 and dis_i = radius of C_{b_p}
Set γ and δ respectively to be the steps of CA and the steps of small
  part within each CA
do
 |  do
 |   |  Estimate e2e delay of a node belongs within the small part of
 |   |    step δ
 |  while for all small parts of step δ within the CA
 |    (dis_i + mγ, dis_i + mγ + 1)
 |  m++
while for all CA within the FoI
Select the maximum e2e delay
```

Fig. 7 *CI* is intersected by FoI

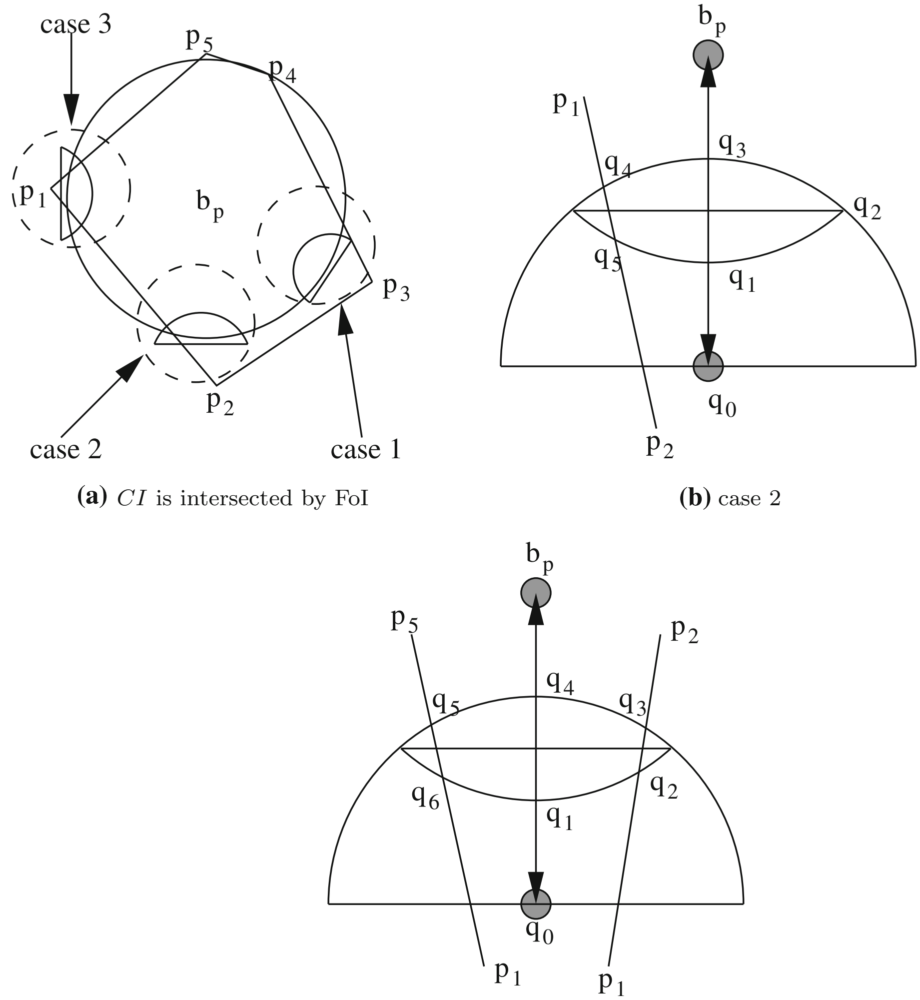

(a) *CI* is intersected by FoI **(b)** case 2

(c) case 3

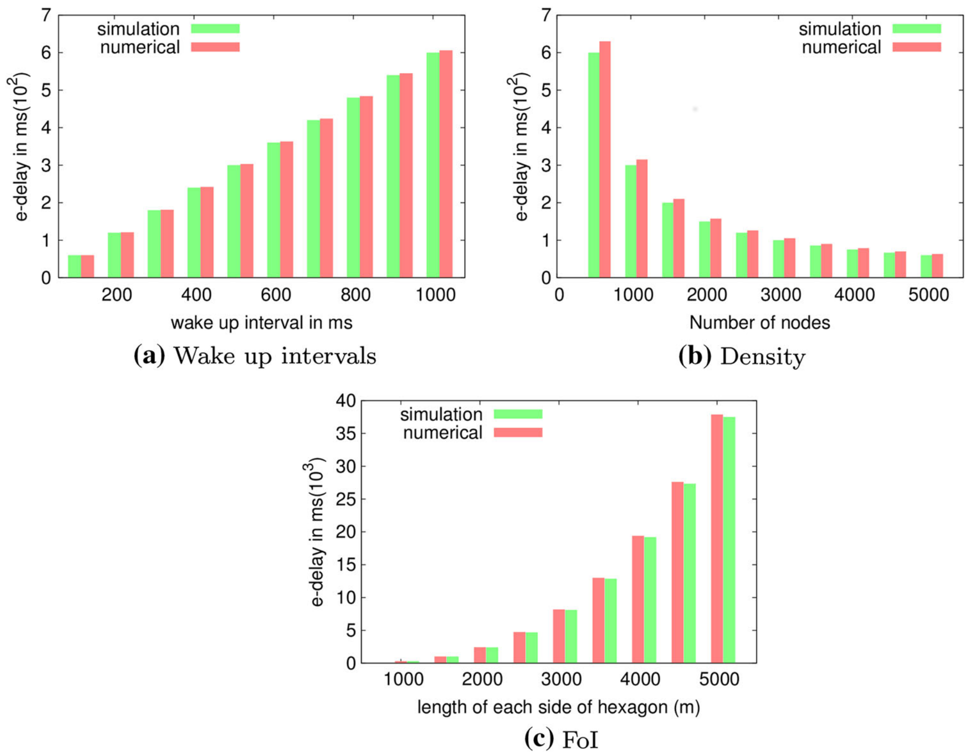

Fig. 8 Validating the estimated expected e2e delay

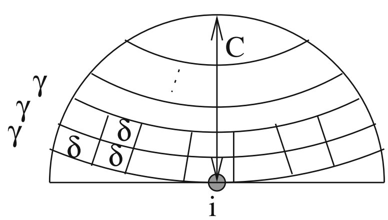

Fig. 9 Shows small parts within circular annulus

3.2 Validation of the analysis using Monte-Carlo simulation

In order to validate our analysis, in this subsection we numerically evaluate the expected e2e delay obtained from Algorithm 2 for given density and wake-up rate, and compare with the Monte Carlo simulation results. We uniformly deploy 200 nodes with communication range of 100 m in a $1000 \times 1000\,\mathrm{m}^2$ area, and calculate the e2e delay from the farthest node in each experiment. We repeat such experiment and change the uniform distribution seed. The average e2e delay of the farthest node is estimated in each experiment. Several tests are carried out in each experiment. In these tests, the receivers' wake up times and the time when the critical event is generated at the farthest node are picked from a set of uniformly distributed random numbers within the wake-up interval. The base-station is placed at the center of the FoI. The experiment is repeated for 100 times. The numerical estimation along with the simulation results are shown in Fig. 8. It is noticed that the simulation results are close to our numerical estimation for various scenarios, though the error bars are not visible.

Wake up interval In Fig. 8(a), we show the average e2e delays for a variety of wake-up intervals. When the wake up interval increases, expected waiting time before sending a packet increases as well which even increases e2e delay. Also note that the estimated expected e2e delay is always higher than the average e2e delay obtained from the simulation.

Density Assuming fixed wake-up interval of 500 ms, average e2e delays are given in Fig. 8(b) for different density. Here, we vary the total nodes the FoI while showing the corresponding average e2e delays. If nodes in the forwarding set increases, one-hop delay decreases and that even may decrease the expected e2e delay. Though the difference in simulation and numerical estimation decreases as we increase the density, but the overall percentage of the over estimation for the expected e2e delay remains almost similar.

FoI In Fig. 8(c), we fix the wake-up interval, and show average e2e delays for various size of FoI. We choose a hexagonal FoI having equal length sides and vary each side of the hexagon to increase the the overall area of FoI (refer Fig. 8c). Note that if we increase the size of the FoI, a packet is expected to traverse more number of hops before reaching to the base-station. This phenomenon increases average e2e delay.

3.3 Minimum cost network for lifetime and delay constraint

In this subsection, we first estimate the minimum cost network for an arbitrary A_i and then use this to estimate overall minimum cost network of the FoI.

3.3.1 Minimizing the network cost for A_i

Consider an area A_i. We first find the e2e delay of A_i for a density. In other words, assuming an arbitrary density λ_a, we can estimate the expected e2e delay of A_i using Sect. 3.1. The network cost of the area A_i is $||A_i|| \times \lambda_a \times c$ where $||A_i|| \times c$ denotes the total number of sensors deployed in A_i an c denotes the cost of each sensor. Note that the density needs to be increased if the expected e2e delay D_e in the area is greater than the delay constraint D_i. In this subsection, our objective is to find the CSD λ_i for A_i that minimizes the deployment cost for A_i.

We define the minimum sensor density, λ_m, as the required density that satisfies the requirement for the coverage constraint. Note that, λ_m can be estimated following the similar methods discussed in [20, 29, 30]. We estimate the CSD, λ_i, required that satisfies the given lifetime requirement L_c and delay constraint D_i by formulating the problem as following.

$$\begin{aligned}
&\min_{\lambda_i} \{||A_i|| * \lambda_i * c\} \quad \textit{subject to} \\
&D_e \leq D_i, \lambda_m \leq \lambda_i, \;\; L_c = \frac{Q}{wE}, \;\; \textit{and} \\
&D_e, L_c, \lambda_i, Q, w, E > 0.
\end{aligned} \tag{11}$$

To estimate an upper bound λ_u for CSD which ensures the lifetime requirement L_c and the delay constraint D_i, assuming the average wake up rate $w = \frac{Q}{LE}$,[6] the density λ_i is exponentially increased from λ_m and we find λ_u to satisfy the delay constraint for corresponding area using Sect. 3.1. To find the CSD λ_i that minimizes the cost of sensor deployment in A_i, we use binary search between λ_u and $\frac{\lambda_u}{2}$.

3.3.2 Minimum cost network

The convex shaped FoI consists of n regions with delay constraint D_i for region A_i, for $1 \leq i \leq n$ (see Fig. 2), such that A_i is closer to the base-station than A_j if $i < j$ for $1 \leq i < j \leq n$. In order to find the overall minimum cost network, we first estimate the CSD λ_1 for A_1 first, then the CSD λ_2 for A_2 is estimated, and so on. To find the minimum cost network, we find the CSD λ_i, for each A_i, for $1 \leq i \leq k-1$, using Algorithm 1, and for the area A_k, λ_k can be found using the method described in Sect. 3.1.3.

3.4 Effectiveness of our approach

In this sub-section, we show the effectiveness of our approach by providing a theoretical analysis. We derive expressions for the expected cost saving and the probability of satisfying delay constraint by a packet.

3.4.1 Expected cost saving

In this sub-section, we compare our approach with uniform critical density (UCD) approach and derive expressions for the expected cost saving in our approach. In Sect. 4.2, we simulate our approach and compare with UCD to show the cost saving using NS2 simulation. In UCD, we fix the uniform density across the FoI that satisfies given delay and lifetime constraints in all areas. In other words, in UCD approach, we deploy the nodes across all the areas A_i, for $1 \leq i \leq n$, with same density. Moreover, we also assume that A_i is closer to the base-station than A_j if $i < j$. In other words, A_1 is the closest area, A_2 is the second closest area, and so on (refer Fig. 2). Assume $||A_i||$ denotes the area associated with A_i and can be denoted using the following expression.

$$\begin{aligned}
||A_i|| &= \pi r_i^2, \quad \text{if } A_i \text{ is circular and } i = 1, \\
&= \pi r_i^2 - \pi r_{i-1}^2, \quad \text{if } A_i, A_{i-1} \text{ is circular and } i \neq 1, \\
&= \pi r_i^2 - \sum_{j=1}^{i-1} ||A_j||, \quad \text{if } j < i \text{ and } A_j \text{ is non-circular} \\
&\qquad \text{and } A_i \text{ is circular}, \\
&= \frac{1}{2} \times \textit{perimeter} \times \textit{apothem} - \sum_{j=1}^{i-1} ||A_j||, \\
&\quad \text{if } A_i \text{ is regular polygon},
\end{aligned} \tag{12}$$

where r_i denotes the radius of A_i if A_i is circular. Moreover, for simplicity we assume that the FoI is a regular polygon (similar in Fig. 2). Note that, the area associated to a regular polygon is $\frac{1}{2} \times \textit{perimeter} \times \textit{apthem}$.

The delay constraint associated to area A_i is less than A_j when $i < j$. In other words, the delay associated to the area $A_i, D_i < D_j$, the delay associated to the area A_j, when $i < j$. Assume the sensor nodes are deployed in different priority areas in increasing order of distance from the base-station. In other words, sensor nodes are deployed first in area A_1, then in area A_2, and so on, to satisfy delay constraint

[6] The corresponding expected e2e delay associated with a sensor density is estimated using the method described Sect. 3.1.

Table 1 Differentiated QoS Cases

	A_1		A_2		A_3		A_4		A_5		w (s)
Case	D_1	λ_1	D_2	λ_2	D_3	λ_3	D_4	λ_4	D_5	λ_5	
1	1	3057	5	764	25	306	125	122	625	49	10
2	1	1528	5	382	25	153	125	61	625	24	5
3	1	611	5	153	25	61	125	24	625	10	2
4	1	306	5	76	25	31	125	12	625	5	1
5	1	306	6	61	36	20	216	7	1296	2	1
6	1	306	7	51	49	14	343	4	2401	1	1
7	1	306	8	44	64	11	512	3	4096	1	1
8	1	306	9	38	81	8	729	2	6560	0.3	1
9	1	306	10	34	100	7	1000	1	10,000	0.2	1
Radius	$r_1 = 200$ m		$r_2 = 400$ m		$r_3 = 800$ m		$r_4 = 1600$ m		$r_5 = 3200$ m		

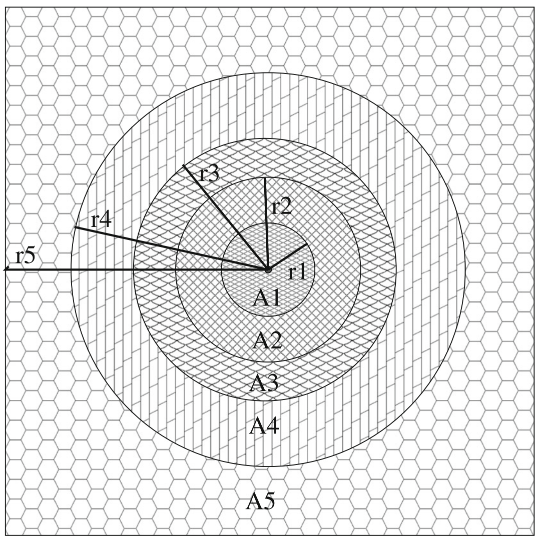

Fig. 10 Simulation scenario

$D_1, D_2, \ldots, D_n$ (refer Fig. 2). Let λ_i denotes the expected CSD in our approach for the area A_i to satisfy delay constraint D_i and lifetime requirement L estimated using the method described in Sect. 3.3. The expected total cost involves in our approach for deployment, $C_{our\_approach}$, can be denoted as

$$C_{our\_approach} = \sum_{i=1}^{n} ||A_i|| \times \lambda_i \times c \tag{13}$$

Note that, if we assume the closest area is with highest priority and with highest density (as in Table 1), then in UCD approach the sensor nodes are deployed across the FoI with the same density as the density required to satisfy delay constraint in the closest area to the base-station. In other words, assuming the closest area has highest density, we denote the expected cost involved in UCD as

Table 2 Simulation parameters

Communication range	100 m
Data rate	19.2 kbps
Transmission power	19.5 mW
Receiving/idle power	13.0 mW
Data packet length	8 bytes
Control packet length	3 byte
Wireless media	802.15.4

$$C_{UCD} = \sum_{i=1}^{n} ||A_i|| \times \lambda_i \times c. \tag{14}$$

Hence, the amount of expected cost saved in our approach compared to UCD is

$$C_s = \sum_{i=1}^{n} ||A_i|| \times \lambda_i \times c - \sum_{i=1}^{n} ||A_i|| \times \lambda_i \times c \tag{15}$$

If the amount of expected cost saved $C_s < 0$ then the expected amount of cost saved in our approach is negative, in other words we incur more cost in our approach. Assuming the closest area to the base-station has the highest priority such that $\lambda_1 \geq \lambda_2 \geq \cdots \geq \lambda_n$, it can be shown that $C_s \geq 0$, which may save the overall expected cost.

3.4.2 Probability of satisfying delay constraint

In this sub-section we compare our approach with uniform density (UD) approach. In UD approach, we deploy the same number of nodes required in our approach uniformly across the FoI. Hence, in the uniform density approach the sensor nodes are deployed using following rate

$$\lambda_{UD} = \frac{\sum_{i=1}^{n} ||A_i|| \times \lambda_i}{\sum_{i=1}^{n} ||A_i||} \tag{16}$$

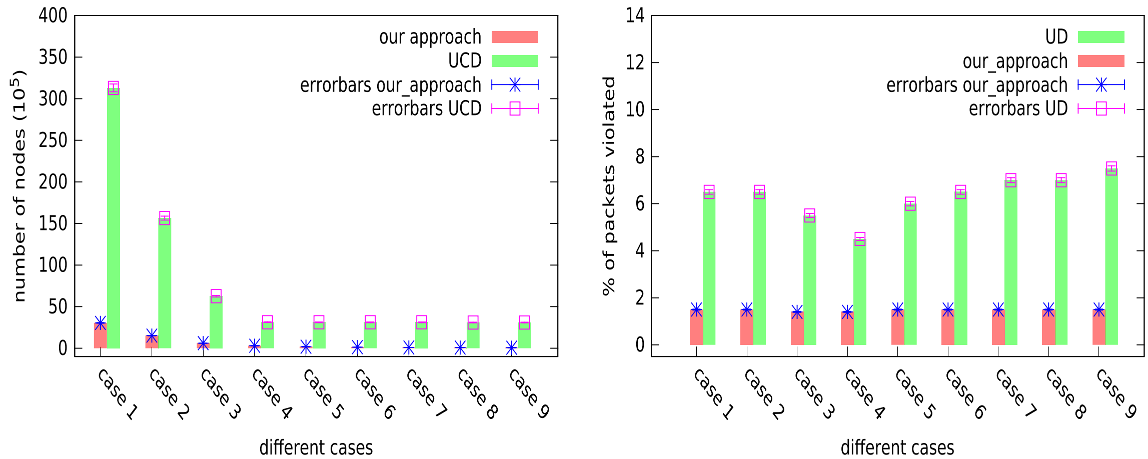

(a) cost

(b) packets violated delay constraint

Fig. 11 Comparing different QoS with other approaches

where, λ_i denotes the density in our approach for A_i. Let D_i^{UD} denotes the expected delay involves in area A_i if the sensor nodes are deployed with rate λ_{UD}. Hence, an area, A_i, is expected to not follow the delay constraint, D_i, if the expected delay involves in uniform density D_i^{UD} is more than D_i. Hence, any packet containing event information generated in these areas is expected to not follow the delay constraint D_i.

Let $X_i \in \{0, 1\}$, for $1 \le i \le n$ denotes the random variable associated with the events that denote whether the delay constraint is satisfied by a packet generated in area A_i. In other words,

$$\begin{aligned} X_i &= 1 \quad \text{if } D_i^{UD} \le D_i \\ &= 0 \quad \text{if } D_i^{UD} < D_i \end{aligned} \tag{17}$$

Assume, a packet containing a critical event information generated in an area A_i satisfies delay constraint D_i if $X_i = 1$ in UD approach, otherwise fails to satisfy delay constraint D_i. Hence, the probability that a packet generated in the FoI follows delay constraint given by

$$P(X) = \frac{\sum_{i=1}^{n} ||A_i|| \times X_i}{\sum_{i=1}^{n} ||A_i||} \tag{18}$$

Assume X denotes the event that a packet containing a critical event information satisfies delay constraint in the FoI. In other words, if $P(X) = 1$ then it implies that all the packets generated follow delay constraints and, $P(X) = 0$ implies that none of the packet follows delay constraint. Note that, in our approach we estimate the critical density that satisfies delay constraint D_i for are A_i, where $1 \le i \le n$. Hence $X_i = 1\ \forall i \in n$ and $P(X) = 1$ in our approach, whereas in UD approach $P(X) \le 1$. In Sect. 4.3, we show the percentage of packets satisfies delay constraint in our approach and UD approach in NS2 simulation.

4 Simulation results

In this section, we show the effectiveness of our approach using NS2 simulation. We assume that the base-station (and the center facility) located in the middle of a square shaped FoI with side length $2\,r_5$. The FoI consists of five different areas A_1, A_2, A_3, A_4, and A_5, defined by radius, r_1, r_2, r_3, r_4, and r_5, as shown in Fig. 10. Moreover, the areas A_1, A_2, A_3, A_4, and A_5, are associated with delay constraints D_1, D_2, D_3, D_4, and D_5, respectively. We consider nine cases as shown in Table 1. The unit for delay constraint and wake-up rate are milliseconds and seconds. The CSD[7] λ_i, for $1 \le i \le 5$, is given in 10^{-3} scale. We can see in Table 1 that if delay constraint increases exponentially, density decreases exponentially as well. This is because, if delay constraint increases in an area, then the number of nodes requires to satisfy the delay constraint decreases which in-turn decreases the density. It can also be noted that, if wake-up interval decreases, density decreases as well. This is because, decreasing wake-up interval decreases expected e2e delay. Hence, the number of nodes requires to satisfy delay constraint can be decreased if we decrease the wake-up interval. Hence, density decreases when wake-up interval decreases for a fixed delay constraint in an area. We also assume that the sensor nodes follow anycasting forwarding strategy [12]. Other parameters used in the simulation are given in Table 2.

[7] The CSD is the average number of sensors present in each m^2 area.

Fig. 12 Density for differentiated QoS cases

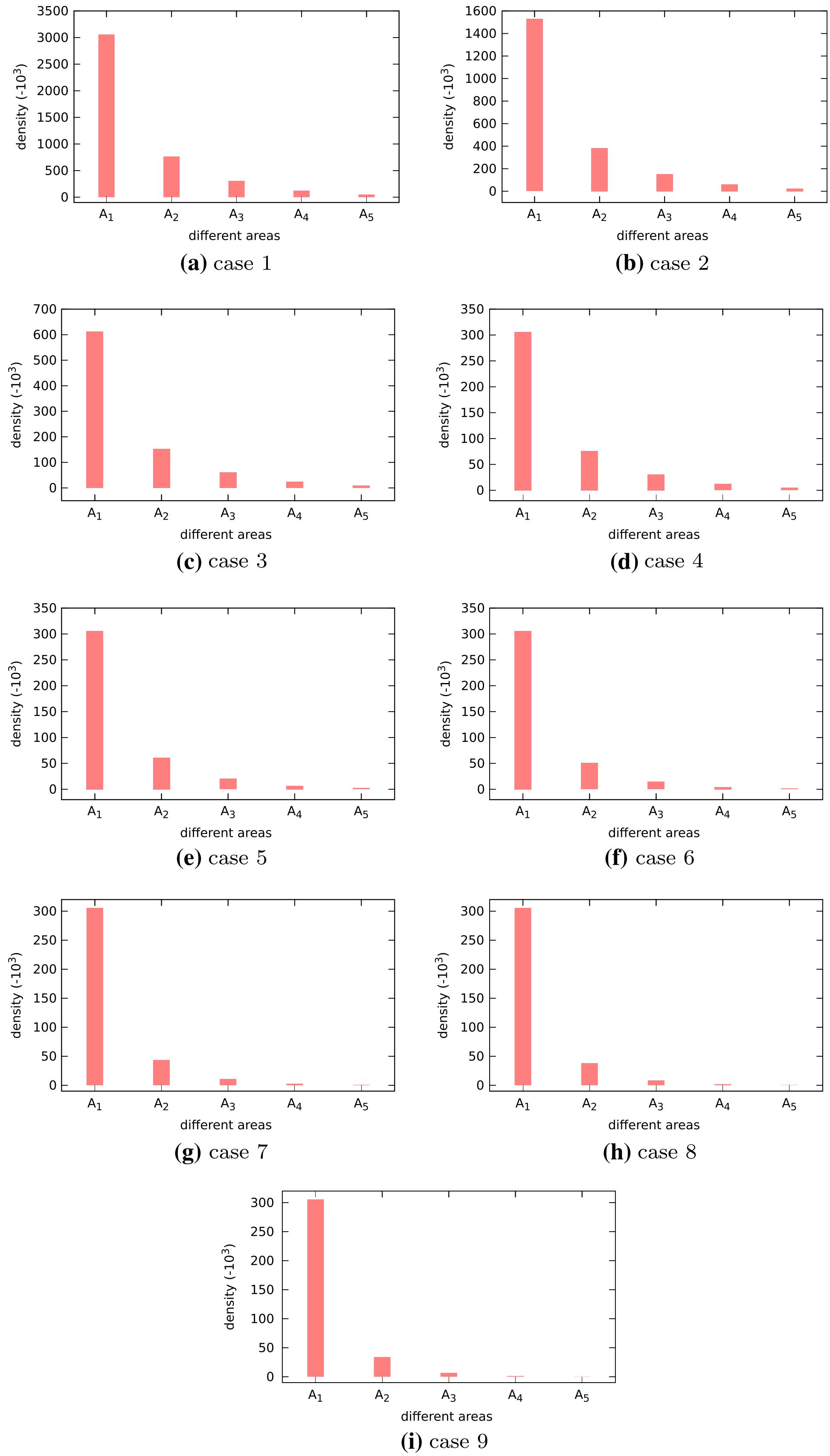

4.1 Densities vesus delay constraint

Here we show that there exist substantial difference in densities for given delay constraints. Different CSDs for different cases are shown in Fig. 12. If the delay increases, density decreases exponentially. This is because, if density decreases, one hop delay increases which in turn increases e2e delay. In other words, lower density is sufficient to satisfy higher delay.

It can be noted from Fig. 12(a)–(d) that if the wake-up interval (and the lifetime) decreases, then CSD required to satisfy various constraints decreases as well. If the wake-up interval decreases the one-hop and the e2e delay decreases as well. As a result, for a fixed delay constraint, one can relax the density if wake-up interval decreases. Note that, if the FoI remains same, the rate at which density changes only depends on the rate at which delay constraint changes. This can be observed in Fig. 12(a)–(d), where the rate at which delay constraint increases remains same, even though the wake-up interval decreases. In the contrary, if the rate at which delay constraint changes, increases (refer Fig. 12e–i), the rate at which density changes also increases.

4.2 Minimizing network cost

In order to show the effectiveness in minimizing the cost, we compare the total number of nodes required to satisfy delay and lifetime constraint in our approach with uniform critical sensor density (UCD) approach, and the results are given in Fig. 11(a) with 95% confidence. We fix the uniform density across the FoI that satisfies given delay and lifetime constraints in all areas in UCD approach. Note that, if we assume the closest area is with highest priority (as in Table 1), then in UCD approach the sensor nodes are deployed across the FoI with the same density as the density required to satisfy delay constraint in the closest area to the base-station.

It can be observed from Fig. 11(a) that our approach minimizes the total number of nodes significantly in all cases. Moreover, cost saving in our approach increases for a higher lifetime requirement. This is because, for a higher lifetime requirement wake-up interval increases which in turn increases expected one hop and e2e delay. Hence, for a fixed delay constraint, density must be increased to satisfy given lifetime requirement. In addition, if the wake-up interval increases, the rate at which density changes across all areas, increases as well. Hence, cost saving in our approach is higher for higher wake-up interval if other parameters are fixed. Also note that, if the rate of change of delay constraint increases, our approach reduces cost further. This is because if this rate increases, the difference in the density increases which can be seen in Fig. 12(d)–(i).

4.3 Satisfying delay and lifetime constraint

We fix the number of nodes and show the effectiveness in satisfying delay and lifetime constraints in our approach. In order to compare the results, we deploy the same number of nodes using uniform density across the FoI and show the percentage of packets violated the delay constraint if wake-up interval (for given lifetime constraint) is fixed. The results are shown in Fig. 11(b) with 95% confidence. Compared to uniform density, our approach performs better in satisfying delay constraints.

5 Conclusion and future work

In this work, we minimize the overall cost of the network with spatially differentiated delay constraint and lifetime requirement. Saving in the network cost using our approach is higher for a higher lifetime requirement and a higher rate of change of delay constraint. Moreover, our analysis can be extended to 3-dimensional heterogeneous WSNs with different communication range. In this work, we assumed a single base-station located at the center facility. Whereas, it would be interesting to extend our work to find a cost efficient network with multiple base-stations.

Acknowledgements We would like to thank department of Computer Science and Engineering, Indian Institute of Technology Guwahati for providing us all the facilities to carry out the research. We would also acknowledge MHRD for their funding for the work.

References

1. AlSkaif, T., Bellalta, B., Zapata, M. G., & Ordinas, J. M. B. (2017). Energy efficiency of mac protocols in low data rate wireless multimedia sensor networks: A comparative study. *Ad Hoc Networks*, *56*, 141–157.
2. Biswas, S., & Morris, R. (2005). Exor: Opportunistic multi-hop routing for wireless networks. *ACM SIGCOMM Computer Communication Review*, *35*(4), 133–144.
3. Cai, H., Jia, X., & Sha, M. (2011). Critical sensor density for partial connectivity in large area wireless sensor networks. *ACM Transactions on Sensor Networks (TOSN)*, *7*(4), 35.
4. Chen, X., Ma, M., & Liu, A. (2017). Dynamic power management and adaptive packet size selection for iot in e-healthcare. *Computers and Electrical Engineering*, *65*, 357–375.
5. Chen, Z., Ma, M., Liu, X., Liu, A., & Zhao, M. (2017). Reliability improved cooperative communication over wireless sensor networks. *Symmetry*, *9*(10), 209.
6. Dorling, K., Messier, G. G., Valentin, S., & Magierowski, S. (2015). Minimizing the net present cost of deploying and operating wireless sensor networks. *IEEE Transactions on Network and Service Management*, *12*(3), 511–525.

7. Ghaffarzadeh, H., & Doustmohammadi, A. (2014). Two-phase data traffic optimization of wireless sensor networks for prolonging network lifetime. *Wireless Networks*, *20*(4), 671–679.
8. Hammoudeh, M., Al-Fayez, F., Lloyd, H., Newman, R., Adebisi, B., Bounceur, A., et al. (2017). A wireless sensor network border monitoring system: Deployment issues and routing protocols. *IEEE Sensors Journal*, *17*(8), 2572–2582.
9. Huang, M., Liu, A., Wang, T., & Huang, C. (2018). Green data gathering under delay differentiated services constraint for internet of things. *Wireless Communications and Mobile Computing*
10. Jang, B., Lim, J. B., & Sichitiu, M. L. (2008). As-mac: An asynchronous scheduled mac protocol for wireless sensor networks. In *Proceedings of the 5th IEEE international conference on mobile ad hoc and sensor systems* (pp. 434–441). IEEE.
11. Jang, U., Lee, S., & Yoo, S. (2012). Optimal wake-up scheduling of data gathering trees for wireless sensor networks. *Journal of Parallel and Distributed Computing*, *72*(4), 536–546.
12. Kim, J., Lin, X., Shroff, N., & Sinha, P. (2010). Minimizing delay and maximizing lifetime for wireless sensor networks with anycast. *IEEE/ACM Transactions on Networking*, *18*(2), 515–528.
13. Kim, J., Lin, X., & Shroff, N. (2011). Optimal anycast technique for delay-sensitive energy-constrained asynchronous sensor networks. *IEEE/ACM Transactions on Networking*, *19*(2), 484–497.
14. Lazos, L., & Poovendran, R. (2006). Stochastic coverage in heterogeneous sensor networks. *ACM Transactions on Sensor Networks (TOSN)*, *2*(3), 325–358.
15. Liu, A., Chen, Z., & Xiong, N. N. (2018a). An adaptive virtual relaying set scheme for loss-and-delay sensitive wsns. *Information Sciences*, *424*, 118–136.
16. Liu, S., Fan, K. W., & Sinha, P. (2009). Cmac: An energy-efficient mac layer protocol using convergent packet forwarding for wireless sensor networks. *ACM Transactions on Sensor Networks (TOSN)*, *5*(4), 29.
17. Liu, Y., Ota, K., Zhang, K., Ma, M., Xiong, N., Liu, A., et al. (2018b). Qtsac: An energy-efficient mac protocol for delay minimization in wireless sensor networks. *IEEE Access*, *6*, 8273–8291.
18. Luo, H., Wu, K., Guo, Z., Gu, L., & Ni, L. M. (2012). Ship detection with wireless sensor networks. *IEEE Transactions on Parallel and Distributed Systems*, *23*(7), 1336–1343.
19. Mitton, N., Simplot-Ryl, D., & Stojmenovic, I. (2009). Guaranteed delivery for geographical anycasting in wireless multi-sink sensor and sensor-actor networks. In *Proceedings of IEEE INFOCOM 2009* (pp. 2691–2695). IEEE.
20. Paillard, G., Ravelomananana, V. (2008). Limit theorems for degree of coverage and lifetime in large sensor networks. In *Proceedings of the 27th conference on computer communications*. IEEE.
21. Rossi, M., & Zorzi, M. (2007). Integrated cost-based mac and routing techniques for hop count forwarding in wireless sensor networks. *IEEE Transactions on Mobile Computing*, *6*(4), 434–448.
22. Rossi, M., Zorzi, M., & Rao, R. R. (2008). Statistically assisted routing algorithms (sara) for hop count based forwarding in wireless sensor networks. *Wireless Networks*, *14*(1), 55–70.
23. Salim, A., Osamy, W., & Khedr, A. M. (2014). Ibleach: Intra-balanced leach protocol for wireless sensor networks. *Wireless Networks*, *20*(6), 1515–1525.
24. Sun, Z., Wang, P., Vuran, M. C., Al-Rodhaan, M. A., Al-Dhelaan, A. M., & Akyildiz, I. F. (2011). Bordersense: Border patrol through advanced wireless sensor networks. *Ad Hoc Networks*, *9*(3), 468–477.
25. Tang, J., Liu, A., Zhao, M., & Wang, T. (2018). An aggregate signature based trust routing for data gathering in sensor networks. *Security and Communication Networks*
26. Yadav, S., & Yadav, R. S. (2016). A review on energy efficient protocols in wireless sensor networks. *Wireless Networks*, *22*(1), 335–350.
27. Yang, T., Mu, D., Hu, W., & Zhang, H. (2014). Energy-efficient border intrusion detection using wireless sensors network. *EURASIP Journal on Wireless Communications and Networking*, *1*, 46.
28. Yen, L., Yu, C., & Cheng, Y. (2006). Expected k-coverage in wireless sensor networks. *Ad Hoc Networks*, *4*(5), 636–650.
29. Zhang, H., & Hou, J. (2004). On deriving the upper bound of alpha-lifetime for large sensor networks. In *Proceedings of the 5th ACM international symposium on mobile ad hoc networking and computing* (pp. 121–132). ACM.
30. Zhang, H., & Hou, J. (2006). Is deterministic deployment worse than random deployment for wireless sensor network? In *Proceedings of IEEE INFOCOM* (pp. 1–13). IEEE.
31. Zhao, Y., Wu, J., Li, F., & Lu, S. (2010). VBS: Maximum lifetime sleep scheduling for wireless sensor networks using virtual backbones. In *Proceedings of IEEE INFOCOM* (pp. 1–5). IEEE.

Debanjan Sadhukhan He received Bachelor of Technology from the West Bengal University of Technology, India. He received Ph.D. in Computer Science and Engineering from the Indian Institute of Technology Guwahati, India. His research interests include wireless sensor networks, wireless ad hoc networks, wireless communication, and distributed algorithms.

Seela Veerabhadreswara Rao He received his Ph.D. in Computer Science Engineering from the Indian Institute of Technology Kanpur, in 1999. Presently, he is the Professor in the Department of Computer Science and Engineering, Indian Institute of Technology Guwahati, India. His research interests include wireless sensor networks, wireless ad hoc networks, data center networks, cloud computing, software defined networks and computational geometry.